VERSITA

Photo-induced superhydrophilicity of nanocomposite TiO_2–SiO_2 thin film

AKBAR ESHAGHI[1*], AMIR DASHTI[2], AMENEH ESHAGHI[3], REZA MOZAFFARINIA[1]

[1]Faculty of Materials Science and Engineering, Maleke Ashtar University of Technology, Shahinshahr, Iran

[2]Department of Mechanical Engineering, Sarvestan Branch, Islamic Azad University, Sarvestan, Iran

[3]Sari Branch, Islamic Azad University, Sari, Iran

In this work, TiO_2 and TiO_2–SiO_2 thin films on glass substrates were prepared by the sol–gel dip coating process. X-ray diffraction (XRD), Fourier transform infrared spectroscopy (FTIR) and X-ray photoelectron spectroscopy (XPS) were used to evaluate the structural and chemical properties of the films. The super-hydrophilicity was assessed by water contact angle measurement. XRD measurements confirmed the presence of polycrystalline anatase and rutile phases in the films. The water contact angle measurements showed that addition of SiO_2 has a significant effect on the super-hydrophilicity of TiO_2 thin films, especially if they are stored in a dark place.

Keywords: *sol-gel, thin film, TiO_2, super-hydrophilicity*

1. Introduction

Super-hydrophilicity is a phenomenon that occurs when TiO_2 film is irradiated with UV irradiation. A very small contact angle appears on the hydrophilic surface ($\theta \leq 5°$). Water tends to spread completely across this surface, rather than forming droplets. This makes the surface particularly suitable for anti-fog applications and easy-washing requirements [1–7]. Super-hydrophilic TiO_2 films on glass substrates are widely used for various applications, such as for mirrors, window glasses, light bulbs, windshields of automobiles, etc [8–10].

Many investigators have studied the super-hydrophilic mechanism of TiO_2 [11–18]. When TiO_2 is irradiated with UV light ($\lambda < 380$ nm), the electrons and holes are produced in conduction and valence bands, respectively. The electrons reduce the Ti(IV) cations to the Ti(III) state, and the holes

oxidize the O^{2-} anions. In this process, oxygen atoms are ejected and oxygen vacancies are created. Water molecules then occupy oxygen vacancies, producing adsorbed OH groups, which tend to make the surface hydrophilic.

If TiO_2 film is stored in a dark place, the surface of TiO_2 is converted to a hydrophobic state. Regeneration of the hydrophobic surface is due to either adsorption of organic contaminants or by release of water molecules, which can be due to the adsorption of oxygen molecules, creating a hydrophobic surface [18]. Therefore, it is desirable that super-hydrophilicity of TiO_2 be maintained for a long time, if storage is in a dark place. In practical applications, the irradiation UV light on the TiO_2 surface does not always occur. Machida [19] indicated that the formation of TiO_2–SiO_2 composite film (10 – 30 mol% SiO_2), maintains the hydrophilicity of TiO_2 in a dark place, for a long time. In the present study, TiO_2 and TiO_2–SiO_2 composite thin films were prepared by the sol-gel dip coating method on glass substrates. The super-hydrophilic

---
*E-mail: eshaghi.akbar@gmail.com

properties of these thin films were then investigated.

2. The Experimental

2.1. Preparation of nanocomposite TiO$_2$–SiO$_2$ thin film

2.1.1. TiO$_2$ sol preparation

The TiO$_2$ precursor sol was prepared by dissolving tetrabutyl orthotitanate (1 mol, Sigma Aldrich, purity 97%) in absolute ethanol (20 mol, Merck, purity $\geq$ 99.5%) and acetyl acetone (0.2 mol, Sigma Aldrich, purity $\geq$ 99%). Acetic acid (1.5 mol, Sigma Aldrich, purity $\geq$ 99.7%) was dissolved in deionized water (3 mol) and absolute ethanol (20 mol), and then added to the first solution during stirring. Each solution was firstly mixed for half an hour and then mixed ultrasonically for half an hour. Acetyl acetone was added to slow the speed of hydrolysis and condensation reactions, thereby promoting the formation of a stable sol.

2.1.2. SiO$_2$ sol preparation

Tetraethylorthosilicate (1 mol, Sigma Aldrich, purity $\geq$ 99.0%) was dissolved in a solution containing absolute ethanol (20 mol) and deionized water (3 mol). Droplets of hydrochloric acid (0.5 mol, Sigma Aldrich, purity 37%) were added to this solution, which was subsequently refluxed at 70 °C for 2 h. The resulting mixture was aged for 24 h, to obtain SiO$_2$ sol.

The precursor solutions were mixed together in a specific quantities. For comparative purposes, sol solutions (films) were prepared from pure TiO$_2$ and from TiO$_2$–SiO$_2$. The molar ratio of TiO$_2$:SiO$_2$ was taken as 4:1.

Before coating, soda-lime glass substrates (75 mm $\times$ 25 mm) were ultrasonically cleaned in acetone and then dipped into an absolute ethanol for 5 min, after which they were thoroughly washed. The thin films were obtained by a dip coating method and deposited at a rate of 5 mm s^{-1}. The gel films were dried in air for 15 h, and were then heat-treated, in air, at 500 °C for 2 h. The dip-coating and heat-treating steps were repeated several times to obtain the desired film thickness. This procedure was carried out three times.

In addition, the pure TiO$_2$ and TiO$_2$–SiO$_2$ composite powder samples were prepared separately, using the described thin film preparation method. TiO$_2$ and TiO$_2$–SiO$_2$ composite gels were prepared by drying the initial solutions at 80 °C for 3 h. Then, the powder samples were prepared by annealing the gels at 500 °C for 2 h in air. The structure of the powder samples was analyzed by using a Bruker X-ray diffractometer (D8ADVANCE, Germany, Ni-filter, CuK$_\alpha$ radiation λ = 1.5406 Å). The chemical properties of the films were characterized by Fourier transform infrared spectroscopy (JASCO FT/IR-689 Plus).

Surface analysis was performed by X-ray photoelectron spectroscopy (XPS) using a MgK$_\alpha$ source (1253.6 eV). The X-ray source was operated at 10 kV under a current of 10 mA. Spectra were calibrated with respect to the O 1s peak at 284.6 eV [17].

The O 1s peak for the films was deconvolved using a Gaussian-20% Lorentzian function, after subtraction of the background by the Shirley method.

The photo-induced super-hydrophilicity of the films was evaluated by measuring the contact angle of water droplets on the film surfaces (environmental condition; T = 25 °C and %H =%37). A droplet was injected on to the surface using a 1 µl micro-injector (Kyowa Interface Science, Drop Master 500). The water contact angle was taken as the average angle from five measurements. UV-Vis was irradiated onto the surface of the samples, using an Xe lamp (power 300 W, wavelength 300 – 500 nm). Before photo-induced super-hydrophilicity measurement were taken, the relevant samples were firstly oven-dried at 100 °C for at least 12 h before. In addition, hydrophilic–hydrophobic conversion of films after storage in a dark place was investigated (environmental condition; T = 21 °C and %H =%31).

3. Result and discussion

3.1. Thickness of the films

The average thicknesses of the films were calculated according to Guan's method [20]. Results indicated that the thicknesses of the pure TiO_2 and TiO_2–SiO_2 films were approximately 215 nm and 198 nm, respectively.

3.2. X-ray diffraction analysis

The powder XRD patterns of the films are shown in Fig. 1. As can be seen, a strong peak occurs for both films at $2\theta = 25.3°$, and which corresponds to the (101) reflection, while the peaks at 37.9°, 48.0°, 54.6° and 62.8° correspond to the (103, 004 and 112), (200), (105 and 211) and (204) crystal planes. The peaks confirm the presence of anatase phase in the films [21, 22]. Also a weak peak occurs for both samples at $2\theta = 27.4°$, which corresponds to the (110) crystal plane. This peak confirms the presence of rutile phase in the films [23].

Therefore, XRD measurements show that both anatase and rutile phases are present in both the pure and the composite, TiO_2–SiO_2 thin films. Furthermore, the XRD patterns for the TiO_2–SiO_2 film do not reveal any additional phases, other than those observed for TiO_2 film. This indicates that chemical interaction between TiO_2 and SiO_2 does not occur. Using the XRD data, the percentage of anatase phase can be calculated using Eq. (1):

$$\% \text{ of anatase phase} = \frac{100}{1 + \frac{I_R}{0.79 I_A}} \quad (1)$$

where, I_A and I_R are the strongest intensities of anatase phase along (101) plane and rutile phase along (110), respectively [24]. The percentage of anatase phase in pure TiO_2 and TiO_2-SiO_2 films was 97% and 91%, respectively. The average crystallite size of anatase phase of the films was calculated from the Scherrer equation [25], using the (101) peak:

$$t = \frac{K\lambda}{\beta \cos\theta} \quad (2)$$

where t is the grain size, K is a constant (0.94), λ is the wavelength of the X-ray ($CuK\alpha - 1.5406$ Å), β
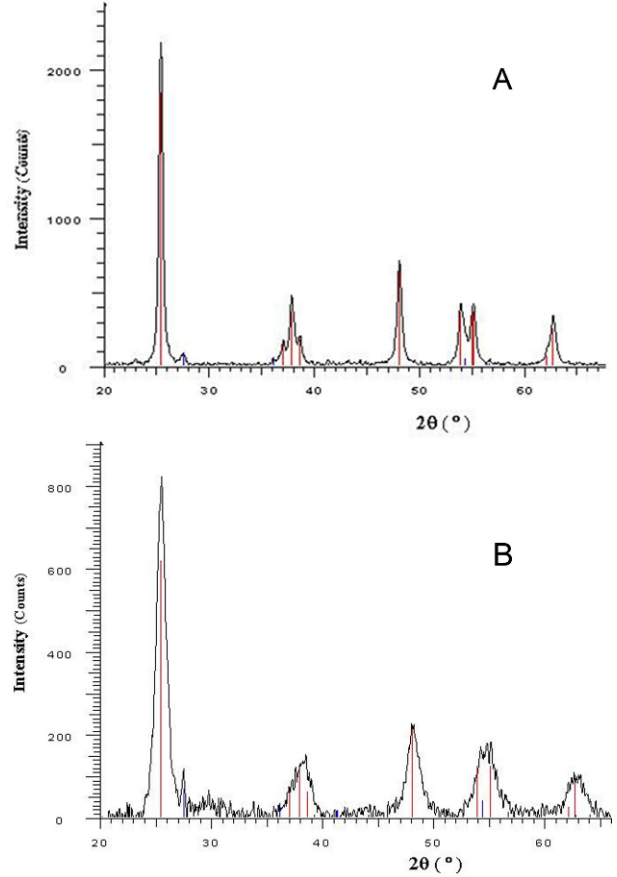

Fig. 1. XRD patterns of powder samples (A) pure TiO_2 and (B) TiO_2–SiO_2.

is the true half-peak with, and θ is the half diffraction angle in degrees. For the TiO_2–SiO_2 thin film, the XRD peak gradually becomes broader. It means that the crystalline size of anatase TiO_2 becomes smaller by the formation of composite film. In the TiO_2–SiO_2 film, the size of crystallites was smaller than in the pure TiO_2. In the pure TiO_2 film, the average crystallite size was 14.6 nm, whereas in the mixed oxide sample TiO_2–SiO_2 film, the average size was 6.8 nm. Moreover, Yu et. al [26] indicated that the addition of additives to titania had a suppressive effect on the crystal growth of TiO_2, since the additives hindered contact between TiO_2 particles and inhibited grain growth during the heat treatment.

3.3. FTIR results

The characterization of the functional groups on the film is important, in order to understand the photo-induced super-hydrophilicity on the surface. Transmission spectra of the films were measured in the range of $4000 - 400$ cm^{-1} with a resolution of 4 cm^{-1}. Fig. 2 shows FTIR spectra for the TiO$_2$–SiO$_2$ film. The adsorption band at about 3400 cm^{-1} is assigned to the stretching modes of O–H bonds and is related to surface absorbed water. The adsorption band at 1600 cm^{-1} is attributed to the bending vibration of H–O–H bonds, which is assigned to the chemisorbed water [27].
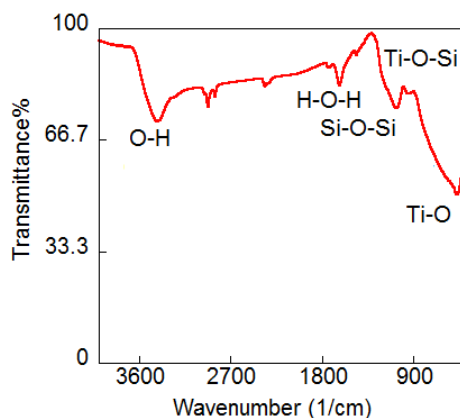

Fig. 2. FTIR spectra of composite TiO$_2$–SiO$_2$ film.

The adsorption band at about 1050 cm^{-1} is assigned to the stretching vibration of Si–O–Si band. The Si–O–Ti linkage stretching band appears at about 950 cm^{-1} [28]. The adsorption band at about 450 cm^{-1} is due to the stretching vibrations of Ti–O–Ti and Ti–O, [29].

3.4. Super-hydrophilic properties

Fig. 3 (left) shows the measurements for the water contact angle on the surface of the films during irradiation (300 min), and Fig. 3 (right) shows the corresponding measurements for the film samples that were stored in a dark place (36 h). The water contact angle of pure TiO$_2$ film, after 180 min irradiation, is reduced to 9.8°, but is 0° for the TiO$_2$–SiO$_2$ composite film. After putting the films in a dark place for 36 h, the water contact angle on TiO$_2$ film increases to 30.1°, and increases to 8.9° for

TiO$_2$–SiO$_2$ film, (Fig. 3b). These results indicate that with the addition of SiO$_2$ to TiO$_2$, the super-hydrophilicity is maintained for a long time in a dark place.

The enhanced hydrophilicity of TiO$_2$–SiO$_2$ composite film can be explained as follows: binary metal oxides are well known to have surface acidity. A popular hypothesis is proposed by Tanabe about surface acidity of binary metal oxides. According to this hypothesis, the acidity generation is caused by an excess of a positive (Lewis sites) or negative (Bronsted sites) charge in the structure of binary oxides. The surface acidity in binary oxides: is described completely by Tanabe [30].

In the structure of TiO$_2$–SiO$_2$, TiO$_2$ is the main oxide. In single oxides, the coordination number of Ti is 6 and that of Si is 4, whereas the coordination number of oxygen in the single oxides are 3 and 2, respectively. It is known that TiO$_2$ and SiO$_2$ form single oxide particles in the films [31]. But, it is possible that at the interfaces of TiO$_2$ and SiO$_2$, Si^{+4} ions replace Ti^{+4} ions in the titania structure: this is indicated by the FTIR data, because the signature of Si–O–Ti vibration is present in the FTIR spectrum. This phenomenon causes charge imbalance, which can be calculated according to Pauling's rule 2 [32]: in a stable structure, the total strength of the valency bonds that reach an anion from all its neighboring cations, S, should be equal to the charge of the anion:

$$S = \frac{Z_m}{CN} \tag{3}$$

where CN is the coordination number and Z_m is the charge on the cation. The fundamental idea is that the crystal must be electrically neutral. The strength of the bonds can be calculated as follows: for Ti^{4+} ions, S = 4/6 = +4/6, for Si^{4+} ion, S = +4/4 = +1.

Thus, charge difference for one bond is (+4/6 × 2 + 1) + (-2) = +1/3, and the total charge imbalance for all bonds (four bond) is 4× (+1/3) = +4/3.

In this case, Lewis acidity is present, which is due to the appearance of excessive positive charge. This charge imbalance must be compensated. Therefore, hydroxyl groups are adsorbed on the surface. Fig. 4 clearly indicates this effect.
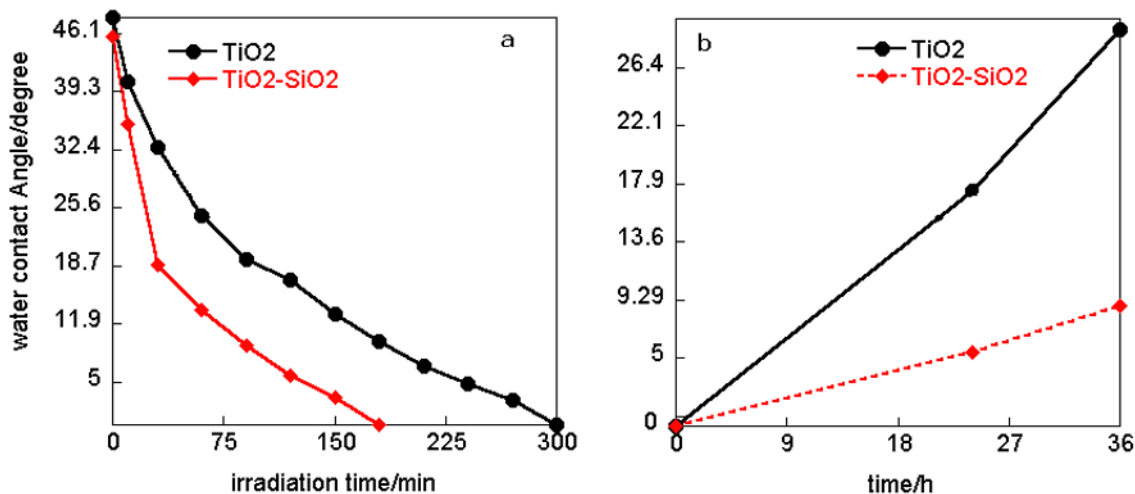
Fig. 3. Water contact angle on film surfaces (a) under irradiation and (b) after storage in a dark place.
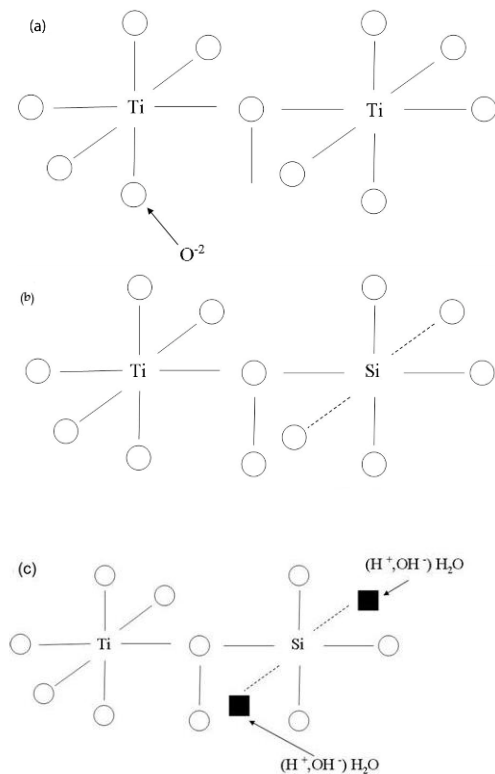

Fig. 4. Hydroxyl group formation, a: TiO_2 structure, b: Si^{+4} ions replace Ti^{+4} ions in titania structure, c: oxygen vacancy generation, adsorption of hydroxyl group.

It is widely accepted that surface acidity and hydroxyl groups are important factors for maintaining superhydrophilicity of TiO_2 thin film, especially when such films are stored in a dark place [20]. XPS is one of the useful methods to measure the amount of hydroxyl groups on the film surface.

Fig. 5 shows the high-resolution XPS spectra for the O 1s region for TiO_2 and the nanocomposite TiO_2–SiO_2 film. The O 1s region is composed of two peaks. One peak is attributed to the Ti–O (529.90 eV) in TiO_2 and the composite film, while the other one is assigned to the hydroxyl group (531.90 eV) [33].

The hydroxyl content for the TiO_2 and TiO_2-SiO_2 nanocomposite film was calculated to be 11.6 and 19.3%, respectively. The hydroxyl content (%) is the ratio of the area of 531.90 eV peak to the total area of the two O 1s peaks.

It is noted that the hydroxyl content in the nanocomposite film is higher than that in TiO_2, which indicates that the amount of the hydroxyl group, arising from the chemisorptions of water molecules on the TiO_2 surface [34], is enhanced by the presence of SiO_2.

Although some water is easily adsorbed on the surface of the samples, the physically adsorbed water on the samples is desorbed under the ultra-high vacuum condition of the XPS system. Therefore, the XPS spectra only show chemisorbed water.
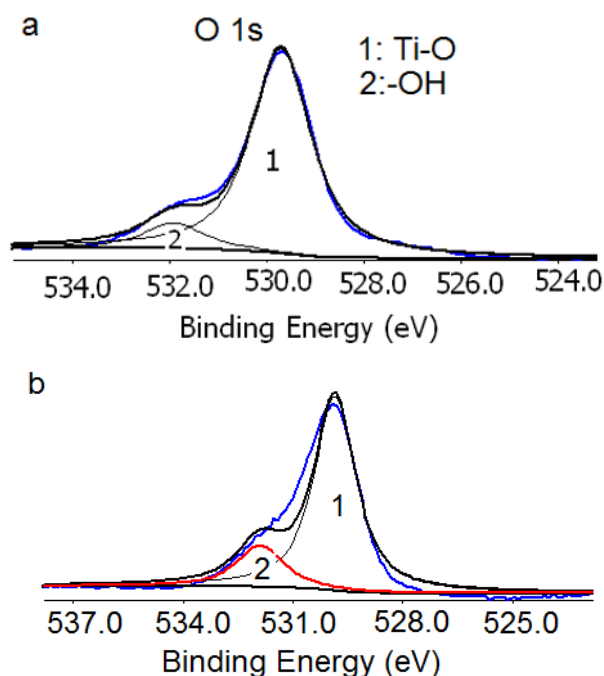
Fig. 5. High-resolution XPS spectra of O 1s region of (a) TiO₂ and, (b) the composite TiO₂–SiO₂.

With the increase of absorbed hydroxyl groups on the surface of composite film, van der Waals forces and hydrogen bond interactions between water molecules and hydroxyl group will increase accordingly. Thus, the increase in the hydroxyl content on the surface of the composite film can enhance the surface wettability and water can easily spread on the surface and hydrophilic property will be enhanced.

In summary, when studying surface acidity it is very important to consider the role played by surface hydroxyl groups. Surface hydroxyl groups are useful to maintaining the hydrophilicity in a dark place.

4. Conclusions

In this work, the effect of SiO_2 addition on the superhydrophilicity of TiO_2 thin films was studied. The results indicated that addition of SiO_2 to TiO_2 has a significant effect on the chemical properties of the surfaces of these films, and on the hydrophilicity of TiO_2 thin film, especially if stor-

age is in a dark place. Therefore, we suggest that nanocomposite TiO_2–SiO_2 sol-gel derived thin film is more useful than TiO_2 film in exhibiting superhydrophilicity, with or without UV/vis radiation, for automobile and industrial applications.

Acknowledgment

References

[1] MENGA F., SUN Z., Appl. Surf. Sci., 1255 (2009), 13.
[2] POMONI K., VOMVAS A., TRAPALIS C., Thin Solid Films., 516 (2008), 1271.
[3] TAGA Y., Thin Solid Films., 517 (2009), 3167.
[4] KAFIZA A., KELLICI S., DARR J.A., PARKIN I.P., J. Photochem. Photobiol. A: Chem. 204 (2009), 183.
[5] DENISSON K.R., BOXALL C., Langmuir., 23 (2007), 4358.
[6] FUJISHIMA A., ZHANG X., C. R. Chimie., 9 (2006),750.
[7] FUJISHIMA A., ZHANG X, TRYK D.A., Surf. Sci. Reports., 63 (2008) ,515.
[8] FUNAKOSHI K., NONAMI T., J. Coat. Technol. Res., 4 (2007) ,327.
[9] NAKAMURA M., Thin Solid Films., 496 (2006),131.
[10] GUAN K., LU B., YINY., Surf. Coat. Technol. 173 (2003) 219.
[11] CHEN J., POON C.S., Build. Environ., 44 (2009), 1899.
[12] SIMONSEN M.E., JENSEN H., LI Z., SOGAARD E.G., J. Photochem. Photobiol. A: Chem. 200 (2008), 192.
[13] OHDAIRA T., NAGAI H., KAYANO S., KAZUHITO H., Surg. Endosc., 21 (2007), 333.
[14] SAKAI N., FUJISHIMA A., WATANABE T., HASHIMOTO K., J. Phys. Chem. B., 105 (2001), 3023.
[15] NOSAKA A.Y., KOJIMA E., FUJIWARA T., YAGI H., AKUTSU H., NOSAKA Y., J. Phys. Chem. B. 107 (2003), 12042.
[16] KONTOS A.I, KONTOS A.G., TSOUKLERIS D.S., VLACHOS G.D., FALARAS P., Thin Solid Films 515 (2007), 7370.
[17] SHARMA S.D, SINGH D., SAINI K.K., KANT C., SHARMA V., JAIN S.C, SHARM C.P., Appl. Catal. A General. 314 (2006) 40-46.
[18] FUJISHIMA A, RAO T.N., TRYK D.A., J. Photochem. Photobiol. C Photochem. Rev. 1 (2000) 1.
[19] MACHIDA M., NORIMOTO K., WATANABE T., HASHIMOTO K., FUJISHIMA A., J. Mater. Sci., 34 (1999), 2569.

[20] GUAN K., YIN Y., Mater. Chem. Phys., 92 (2005), 10.

[21] SREEMANY M., SEN S., Mater. Chem. Phys., 83 (2004) , 169.

[22] SHARMA S.D, SINGH D., SAINI K.K, KANT C., SHARMA V., JAIN S.C, SHARMA C.P., Appl. Catal. A General., 314 (2006), 40.

[23] LUCA D., MARDARE D., IACOMI F., TEODOR-ESCU C.M., Appl. Surf. Sci., 252(2006), 6122.

[24] CHEN J., YAO M., WANG X., J. Nanopart. Res., 10 (2008), 163.

[25] DOSS C.J, ZALLEN R., Phys. Rev. B Condense Mater., 48 (1993), 15626.

[26] YU J., ZHAO X., YU J., ZHONG G., J. Mater. Sci. Lett., 20 (2001), 1745.

[27] TAKEUCHI M., BERTINETTI L., MARATA G., COLUCCIA S., ANPO M., Appl. Catal. A General. 307 (2006), 13.

[28] PARK J.K., KIM H.K., J. Mater. Process. Technol., 186 1-3 (2007), 367.

[29] JENSEN H., SOLOVIEV A., LI Z., SOGAARD E.G., Appl. Surf. Sci., 246 (2005), 239.

[30] TANABE K., SUMIYOSHI T., SHIBATA K., KIYOUR T, J. Bull. Chem. Soc. Japan, 47 (1974), 1064.

[31] EHRMAN S.H., FRIEDLANDER S.K., ZACHARIAH M.R., J. Mater. Res., 14 12(1999), 4551.

[32] CARTER C.B., NORTON M.G., Ceramic Materials; Science and Technology. Springer, 2007.

[33] YU J., YU J.C., HO W., JIANG Z., New J. Chem., 26 (2002), 607.

[34] YU J.C., YU J., HO W., ZHAO J., J. Photochem. and Photobiol. A Chem., 148 (2002) 331.